Hindawi
Advances in Meteorology
Volume 2022, Article ID 9717192, 9 pages
https://doi.org/10.1155/2022/9717192

Research Article

Air Pollutants Sources in Winter in Chang-Zhu-Tan Region of China

Yingfang Zhu,[1,2] **Juyang Liao**,[2,3,4] **Wei Gong**,[1] **Huili Wu**,[1] **Yaqi Huang**,[2,3] **Yan Liu**,[2,3] **and Meifang Zhao**[1]

[1]*College of Science, Central South University of Forestry and Technology, Changsha 410004, China*
[2]*Chang-Zhu-Tan Station for Scientific Observation and Research of Urban Agglomeration Ecosystems, Changsha 410116, Hunan, China*
[3]*Hunan Botanical Garden, Changsha 410116, China*
[4]*Beijing Forestry University, Beijing 10083, China*

Correspondence should be addressed to Juyang Liao; liaojuyang@163.com

Received 12 January 2022; Revised 15 February 2022; Accepted 23 February 2022; Published 25 March 2022

Academic Editor: Upaka Rathnayake

In order to analyze the primary sources of air pollutants in Chang-Zhu-Tan region, this article selected the environmental monitoring data and meteorological data in the winter of 2019 to calculate the backward airflow trajectories with the Chang-Zhu-Tan region as the starting point by using the backward trajectory model. Combined with the ground concentration monitoring data, cluster analysis, potential source contribution factor (PSCF) analysis, and concentration weighted trajectory (CWT) analysis were carried out to determine the pollutant transportation paths and sources of the potential source area. The results show that air mass transportation mainly comes from three directions: northwest, northeast, and southwest China. The airflow in northwest China moves faster and cleaner, while the airflow from the northeast and southwest moves slowly and carries a high concentration of pollutants. PSCF and CWT analyses show that the critical potential sources are mainly located in this area and some cities next to the study area. This study has important practical significance for the environmental research of Chang-Zhu-Tan region and can provide theoretical reference for regional joint prevention and control of air pollution.

1. Introduction

Regional air pollution is caused by human activities and local special geographical location, which has been the most severe environmental problem in recent years [1]. The spatial and temporal distribution characteristics of urban air pollution in China are prominent [2, 3]. In winter, significant disastrous weather is frequent, so air pollution is the most serious, followed by spring and autumn, and summer is the best [4]. Air pollution sources can be divided into two categories, natural and human-made sources. The anthropogenic source is the main aspect of air pollution. It is mainly produced by people's production activities and daily activities (industry, transportation, various combustion, garbage treatment, etc.). The primary pollutants include particulate matter (PM2.5, PM10), carbon monoxide (CO), nitrogen dioxide (NO_2), sulfur dioxide (SO_2), and ozone (O_3) [5]. In most studies, scholars mainly analyzed the spatial-temporal pattern, pollution characteristics, and transportation path of PM2.5. However, there are few studies on the overall analysis of multiple pollutants [6].

The research contents of source analysis of air pollutants mainly include quantitative source analysis, cause and process analysis, and local source inventory analysis [7–18]. In the study of source analysis of air pollutants, some scholars used the constrained positive matrix decomposition method, Kriging interpolation method, positive matrix factorization method, and so forth [7, 8, 19]. HYSPLIT (Hybrid Single-Particle Lagrangian Integrated Trajectory) backward trajectory model is often used to deal with input fields of various meteorological elements and emission sources of different types of pollutants. The source,

transportation, air mass trajectory, diffusion, sedimentation, and other processes of air pollutants are also calculated and analyzed. The possible transmission path from the pollution source to the corresponding recipient area at a specific time is estimated to show the concentration contribution and spatial and temporal distribution characteristics of pollutants [9]. The research methods include trajectory cluster analysis, potential source contribution function (PSCF), and concentration weighted trajectory (CWT). Cluster analysis allocates trajectories into representative spatial groups. PSCF is a conditional probability function, which uses a backward trajectory to describe the geosynchronous orientation of potential sources and identify pollution sources. Because it only calculates the number of pollution trajectories, not the concentration of pollutants, it is difficult to distinguish pollution degrees of different pollution sources. CWT model can produce the difference of pollution trajectory in pollution degrees. Trajectory clustering analysis, PSCF, and CWT have been widely applied in published studies, and their combination can provide better information on the location of pollution sources [8, 9, 13–15, 20].

According to the information released on the website of the Ecology and Environment Department of Hunan, in recent years, Changsha, Zhuzhou, and Xiangtan (Chang-Zhu-Tan) have been at the bottom of Hunan province in the air quality index evaluation ranking. Chang-Zhu-Tan region is one of the national "two-type society" comprehensive reform experimental areas. In recent years, the apparent economic growth makes the task of environmental protection increasingly arduous. In the literature of air pollution source analysis, most of the domestic research areas are concentrated in Beijing-Tianjin-Hebei, Yangtze River Delta, north China, west China, and northwest China [8, 10–12, 15, 16, 20]. There are few related types of research in central China, especially in Chang-Zhu-Tan region [8, 10–12, 15, 16, 20].

In this study, the primary and potential sources of air pollutants in Chang-Zhu-Tan region in winter were studied based on hourly pollutant data by using trajectory cluster analysis, PSCF, and CWT. Our objectives were (i) to analyze the air mass transportation in Chang-Zhu-Tan region and (ii) to determine the pollutant transport path and pollution source of potential source area.

2. Materials and Methods

2.1. Site Description. Chang-Zhu-Tan Urban Agglomeration, including Changsha (28.23°N, 113°E), Zhuzhou (27.83°N, 113.16°E), and Xiangtan (27.87°N, 112.91°E) cities, is located in the central and eastern part of Hunan province in China. The three cities are distributed in the lower reaches of Xiangjiang River in an inclined "*T*" shape. Chang-Zhu-Tan belongs to the subtropical monsoon climate zone, with apparent seasonal variation, cold winter and hot summer, abundant precipitation, suitable temperature, less severe winter, more northwest wind, and vulnerability to cold wave and strong wind. The topography is mainly hills and plains, in which mountains, hills, plains, and rivers are distributed alternately. The terrain is high in the south and low in the north. The north is flat and open, and the south is hilly [21]. The area with an altitude below 100 m accounts for 88.72% of the total area of the study area.

2.2. Data Sources. In this study, the air quality data (mainly the concentration of pollutants) were from the China National Environmental Monitoring Centre. There are 24 ground air quality monitoring points in the study area, as shown in Table 1. The data collection time range was winter of 2019 (December to February of the next year), and the data's resolution was 1 hour. The meteorological data (including air pressure, dew point, wind direction, wind speed, temperature, cloud cover, precipitation, etc.) used in the backward trajectory model were recorded by the global data assimilation system of the United States every six hours, which are 0, 6, 12, and 18 o'clock, respectively [22].

2.3. Data Analysis

2.3.1. HYSPLIT Model. The backward trajectory model represents the latest state of the air mass, and the atmospheric mass trajectory can provide the information of the area affected by the point source. Taking Changsha, Zhuzhou, and Xiangtan as the simulation center, 500 m is selected as the average flow field of the atmospheric boundary layer near the surface of the study area. Based on the HYSPLIT 4 model developed by NOAA (National Oceanic and Atmospheric Administration) and BOM (Australia's Bureau of Meteorology), the 72 h backward airflow trajectories arriving at the research area every 6 hours from December 2019 to February 2020 are calculated. Driven by the global atmospheric reanalysis data of the National Centre for Environmental Prediction (NCEP), the model covers the whole process of transport, diffusion, and deposition and is widely used in pollutant transport path and source area analysis [23].

2.3.2. Trajectory Cluster Analysis. Cluster analysis is a multivariate statistical analysis method that classifies the original data according to their similarity and affinity [20]. The backward trajectory clustering in the HYSPLIT model is to cluster and group all air mass trajectories from the source to the receiving point according to the spatial similarity of air mass movement, including the velocity and direction of movement, to obtain different types of airflow trajectories. Based on the moving direction and velocity, the air mass trajectories in winter in Chang-Zhu-Tan are clustered. The backward trajectories of airflow movement are then classified according to the change rate of total space variance (TSV).

2.3.3. Potential Source Contribution Function (PSCF) Analysis. PSCF is a method based on conditional probability function to calculate and judge the geographical orientation of potential source area and further identify the pollution source area using airflow trajectory [13–15]. The

Table 1: Longitude and latitude of the air quality monitoring points in the study.

Monitoring point	Longitude	Latitude	Monitoring point	Longitude	Latitude
Jingkai district (Changsha)	113.08°E	28.23°N	Jianglu (Xiangtan)	112.89°E	27.87°N
Gaokai district (Changsha)	112.89°E	28.22°N	Yuetang (Xiangtan)	112.92°E	27.82°N
Hunan University of Chinese Medicine (Changsha)	112.89°E	28.13°N	Hunan University of Science and Technology (Xiangtan)	112.91°E	27.91°N
Hunan Normal University (Changsha)	112.94°E	28.19°N	Zhaoshan (Xiangtan)	113.00°E	27.92°N
Yuhua district (Changsha)	113.00°E	28.14°N	Shaoshan (Xiangtan)	112.49°E	27.92°N
Wujialing (Changsha)	112.98°E	28.26°N	Tiantao Hills (Zhuzhou)	113.14°E	27.82°N
New railway station (Changsha)	113.00°E	28.19°N	Zhuye hospital (Zhuzhou)	113.10°E	27.89°N
Tianxin district (Changsha)	112.98°E	28.12°N	No.4 Middle School (Zhuzhou)	113.17°E	27.87°N
Mapoling (Changsha)	113.08°E	28.21°N	Railway station (Zhuzhou)	113.14°E	27.84°N
Shaping (Changsha)	113.00°E	28.36°N	Zhuzhou (Zhuzhou)	113.13°E	27.85°N
Bantang (Xiangtan)	112.94°E	27.86°N	Dajing Scenic Spot (Zhuzhou)	113.25°E	27.83°N
Xiangtan (Xiangtan)	112.91°E	27.84°N	Yuntian Middle School (Zhuzhou)	113.18°E	28.00°N

study area is divided into i grids and calculated according to the formula.

$$\mathrm{PSCF}_i = \frac{M_i}{N_i}, \tag{1}$$

where M_i is the residence time in the i grid of all contaminated air mass tracks whose concentration exceeds the set threshold; N_i is the total residence time of all air mass trajectories in the i grid. The larger the result value, the higher the proportion of pollution tracks passing through the area. The corresponding region is more likely to be the potential source area of pollutants, and the trajectory of high value is the main path of pollutant transport.

2.3.4. Concentration Weighted Trajectory (CWT) Method. PSCF represents the proportion of pollution trajectories in all trajectories in each grid, only reflects the proportion of pollution trajectories, and cannot show the difference of pollution degree of pollution trajectories; that is, it cannot reflect the difference of pollution contribution of different source regions. Furthermore, the CWT of the trajectory can be calculated by using the concentration weighted trajectory analysis method, and the difference of the pollution trajectory in the pollution degree can be obtained to make up for the deficiency of the PSCF method. CWT [20] is used to calculate the weight concentration of trajectories, and the average weight concentration of grids is quantitatively given. The calculation formula is shown as follows:

$$\mathrm{CWT}_i = \frac{1}{\sum_{n=1}^{m} N_{in}} \sum_{n=1}^{m} C_{in}, \tag{2}$$

where CWT_i is the average weight concentration of grid i; n is the trajectory; N_{in} is the residence time of trajectory n in the i grid; m is the number of trajectories; C_{in} is the pollutant mass concentration corresponding to the trajectory n passing through the i grid.

3. Results

3.1. Analysis of Air Mass Transportation in Chang-Zhu-Tan Region. The distribution map of backward airflow trajectories in the winter of 2019 in Chang-Zhu-Tan is drawn, as shown in Figure 1. Obviously, the northwest, northeast, and southwest directions are the main transport directions of airflow in the study area, some of which are similar to the clockwise clover. The movement speed of the airflow is expressed by the length of the trajectory. The air mass moving faster leads to the trajectory longer. It can be seen that the airflow in the northwest direction is relatively rapid, mainly due to the influence of monsoon climate and strong wind.

3.2. Cluster Analysis of the Backward Trajectory. Based on the moving direction and velocity, the air mass trajectories of each month are clustered. The backward trajectories of airflow movement are divided into 3 or 4 categories according to the change rate of TSV value, as shown in Figure 2. The longest track reached about 40°N, and the air mass moved fastest. Compared with the trend of mountains in China, it can be seen that the track was along the Qilian Mountains, passing through the channel between Qinling Mountains and Daba Mountains into central China, passing through Inner Mongolia, Gansu, Shaanxi, Henan, and Hubei provinces and finally arriving at the research area. The trajectory of airflow transport from Hubei, the northern neighbouring province, was the shortest and the moving speed of air mass was slow. Simultaneously, combined with the air pollutant concentration data for statistical analysis, the occurrence probability of each type of trajectory and the corresponding average value of air pollutant concentration (see Table 2) are calculated to analyze the impact of different types of airflow on the concentration of pollutants. In order to facilitate analysis and comparison, the hourly mass concentration data of air pollutants in the winter of 2019 (December 2019 to February 2020) are used to calculate the average concentration of pollutants (see Table 3).

In December 2019, the fastest moving air mass was No. 1 from the north of the study area, passing through Shanxi, Henan, and Hubei, and the probabilities of its occurrence in all tracks in Changsha, Zhuzhou, and Xiangtan were 23%, 34%, and 25%, respectively. In the corresponding pollutant concentration table of the three places, the daily average level of O_3 was lower than the average value of daily average concentration in winter of 2019, and the concentrations of PM2.5, SO_2, NO_2,

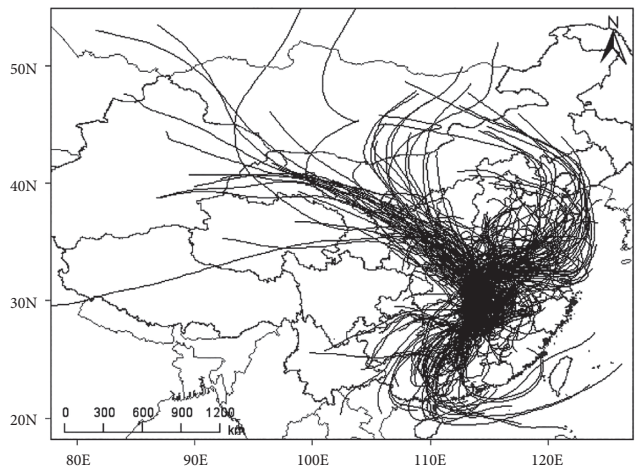

Figure 1: Distribution of backward airflow trajectories from December 2019 to February 2020 in Chang-Zhu-Tan region.

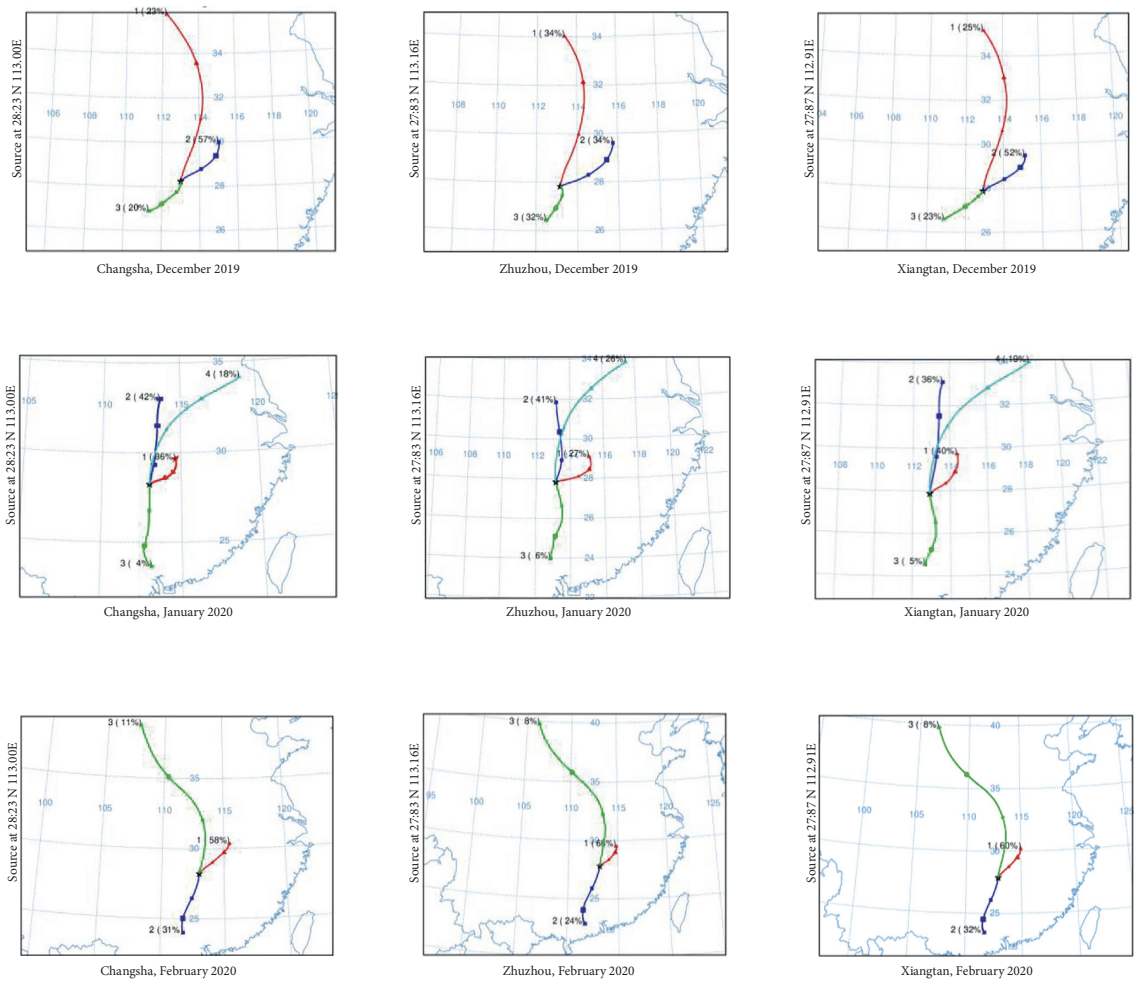

Figure 2: Clustering distribution of backward trajectories from December 2019 to February 2020 in Chang-Zhu-Tan region.

and CO in Changsha and Xiangtan were lower than the average values, and the carrying pollution was light. The concentration of PM10 in Changsha was 54.2 $\mu g/m^3$, close to the average value of 60.26 $\mu g/m^3$, but PM10 in Xiangtan was 70.7 $\mu g/m^3$ and that in Zhuzhou was 82.2 $\mu g/m^3$. It can be seen that Zhuzhou was the highest pollutant concentration affected by the No. 1 airflow trajectory, and the concentrations of SO_2, NO_2, and PM10 were higher than those of the other two cities. The No. 2 airflow trajectory passing through Jiangxi and Hubei provinces was the main transport channel, accounting for 57%, 34%, and 52% of

Table 2: Analysis of various trajectory paths and pollutant concentrations for December 2019 to February 2020 in Chang-Zhu-Tan.

Month	City	Track	Probability (%)	Airflow trajectories area	Average concentration of pollution ($\mu g/m^3$)					
					PM 2.5	PM 10	SO_2	NO_2	O_3	CO
December 2019	Changsha	1	23	Yueyang, Xianning, Western of Wuhan, Xiaogan, Zhumadian, Jincheng	63.5	54.2	7.2	39.7	26.5	1.1
		2	57	Jiujiang, Huangshi	87.4	84.4	8.7	56.6	26.4	1.1
		3	20	Xiangtan, Shaoyang	66.5	61.0	8.7	49.3	24.4	1.1
	Zhuzhou	1	34	Yueyang, Xianning, Western of Wuhan, Xiaogan, Zhumadian, Jincheng	65.2	82.2	10.8	46.9	25.3	0.9
		2	34	Jiujiang, Huangshi	82.0	98.9	12.2	58.2	27.0	1.1
		3	32	Xiangtan, Shaoyang	99.2	121.2	17.3	59.5	23.1	1.2
	Xiangtan	1	25	Yueyang, Xianning, Western of Wuhan, Xiaogan, Zhumadian, Jincheng	66.0	70.7	7.2	42.7	23.8	0.9
		2	52	Jiujiang, Huangshi	90.8	104.1	9.8	56.8	26.9	1.0
		3	23	Xiangtan, Shaoyang	60.7	67.5	11.6	47.6	23.0	1.1
January 2020	Changsha	1	42	Central Hubei, Central Henan	45.3	34.1	4.4	26.3	33.9	1.1
		2	36	Border of northwest Hunan and Hubei, Wuhan	73.4	61.8	5.4	37.8	30.1	1.2
		3	4	Central Hunan, Border of Hunan and Guangdong, Central Guangdong	62.6	53.0	5.6	36.6	20.8	1.3
		4	18	Central Hubei, Border of Hubei and Southern Henan, Border of Henan and Anhui, Border of Shandong and Anhui, Border of Shandong and Jiangsu	49.0	35.2	3.5	14.3	46.6	1.0
	Zhuzhou	1	27	Border of Western Hunan and Jiangxi, Central and Northern of Jiangxi	66.5	76.4	8.3	42.7	20.9	1.0
		2	41	Central Hubei, Central Henan	55.1	60.9	7.5	33.2	33.2	0.9
		3	6	Central Hunan, Border of Southeast Hunan and Guangdong, Central Guangdong	93.6	122.6	10.0	47.4	21.1	1.3
		4	26	Central Hubei, Border of Hubei and Southern Henan, Border of Henan and Anhui, Border of Shandong and Anhui, Border of Shandong and Jiangsu	36.9	34.7	5.3	22.7	33.6	0.8
	Xiangtan	1	40	Border of northwest Hunan and Hubei, Eastern Hubei	72.8	75.4	8.0	41.5	26.4	1.0
		2	36	Central Hubei, Central Henan, Border of Henan and Shansi	42.3	42.5	5.6	27.9	31.6	0.8
		3	5	Central Hunan, Border of Southeast Hunan and Guangdong, Central Guangdong	83.2	92.2	7.8	47.0	17.3	1.1
		4	19	Central Hubei, Border of Hubei and Southern Henan, Border of Henan and Anhui, Border of Shandong and Anhui, Border of Shandong and Jiangsu	46.8	42.7	4.0	19.3	40.1	0.8
February 2020	Changsha	1	58	Border of northeast Hunan and Hubei, Eastern of Hubei	45.6	36.6	4.7	15.0	50.7	0.8
		2	31	Central Hunan, Border of Southeast Hunan and Guangxi, Border of Eastern Guangxi and Guangdong	36.6	39.2	6.3	23.3	41.9	1.0
		3	11	Central Hubei, Border of Western Henan and Shanxi, Border of Shanxi and Shaanxi	15.7	19.9	4.7	6.5	66.3	0.6
	Zhuzhou	1	68	Border of northeast Hunan and Hubei, Southeast of Hubei	40.8	45.8	6.2	19.7	45.4	0.6
		2	24	Central Hunan, Border of Southeast Hunan and Guangxi, Border of Eastern Guangxi and Guangdong	30.6	33.9	8.0	19.9	46.8	0.8
		3	8	Central Hubei, Border of Western Henan and Shanxi, Border of Shanxi and Shaanxi, Border of Northern Shaanxi and Inner Mongolia	11.7	19.4	5.7	9.3	60.6	0.4
	Xiangtan	1	60	Border of northeast Hunan and Hubei, Southeast of Hubei	41.7	43.9	6.1	18.3	45.1	0.7
		2	32	Central Hunan, Border of Southeast Hunan and Guangxi, Border of Eastern Guangxi and Guangdong	37.2	44.2	8.9	25.3	35.3	1.0
		3	8	Central Hubei, Border of Western Henan and Shanxi, Border of Shanxi and Shaanxi, Border of Northern Shaanxi and Inner Mongolia	11.3	17.7	4.8	8.2	58.6	0.5

Table 3: Daily average concentration of pollutants in winter of 2019 in Chang-Zhu-Tan.

Pollution	Daily average concentration ($\mu g/m^3$)	National secondary standard limit
CO	0.93	4
NO_2	34.77	40
SO_2	7.78	150
PM2.5	59.43	75
PM10	60.26	150
O_3	55.70	160

the track probability of Changsha, Zhuzhou, and Xiangtan, respectively. The average concentrations of PM2.5, PM10, SO_2, and NO_2 carried by the airflow were the highest in Changsha and Xiangtan. The impact of the No. 3 airflow trajectory from the south on the concentration of atmospheric particulates corresponding to Changsha and Xiangtan was similar to that of No. 1, and the pollution carried by No. 3 had a more significant impact on Zhuzhou. The corresponding concentrations of PM2.5, PM10, SO_2, and NO_2 reached 99.2, 121.2, 17.3, and 59.5 $\mu g/m^3$, respectively, which were much higher than the average values in winter. No. 1, No. 2, and No. 3 air trajectories had little effect on O_3 and CO, and O_3 concentration was lower than the average level in winter. Among all the trajectories, the No. 2 airflow trajectory had a significant influence on the particulate matter concentration in Changsha and Xiangtan, while the concentrations of other pollutants except O_3 and CO in Zhuzhou were greatly affected by the No. 2 and No. 3 trajectories.

In January 2020, the three cities' backward trajectories were divided into four categories according to the change rate of TSV value. Among them, the first three types of tracks were similar to those of the previous month. The airflow of trajectory No. 4 accounted for 18%, 26%, and 19% of the total tracks of Changsha, Zhuzhou, and Xiangtan, respectively, passing through Henan, Anhui, the border areas of Shandong and Anhui, and the border areas of Shandong and Jiangsu. The air mass moved rapidly with long transmission distance and long trajectory. However, the average concentrations of PM2.5, PM10, SO_2, and NO_2 carried by the airflow were far lower than the seasonal average values; in particular, SO_2 was only between 3.5 and 5.3 $\mu g/m^3$, and the pollution is relatively light. However, compared with other airflow trajectories, the O_3 concentration carried by No. 4 was higher, about 40 $\mu g/m^3$. The concentration of air pollutants carried by the No. 2 airflow track from the north through central Hubei and central Henan was not high. Trajectory No. 3 accounted for the least proportion, accounting for 4%, 6%, and 5% of the total trajectories of Changsha, Zhuzhou, and Xiangtan, respectively. It carried about 1.3 $\mu g/m^3$ of CO through Guangdong to the central part of Hunan, which was higher than other airflow trajectories. The length of the No. 1 airflow trajectory imported from Hubei was relatively short, and the air mass movement speed was not fast. The PM2.5 concentration was about 10 $\mu g/m^3$ higher than the average seasonal value of 59.43 $\mu g/m^3$ and hovered around the national standard daily average concentration limit of 75 $\mu g/m^3$. It may be due to the impact of anthropogenic pollution, and the fine particulate matter pollution was more serious.

In February 2020, the main transport channel was the No. 1 airflow trajectory, accounting for 58%–68% of the total number of tracks. It passed through the eastern part of Hubei and the northeast of Hunan, with a short track and slow-moving air mass speed. The concentration of air pollutants carried except for O_3 by it was lower than the average seasonal value. Perhaps due to the impact of the SARS-CoV-2, during this period, the factory was shut down, and the traffic flow was reduced, so the air pollutants in the area along the route were also significantly reduced. Airflow trajectory No. 2 came from the border of eastern Guangxi and Guangdong and the central and southeast of Hunan. In addition to O_3, the concentrations of input air pollutants were also at a low level. The No. 3 airflow trajectory with the least probability of total trajectories, ranging from 8% to 11%, came from the boundary of northern Shaanxi and Inner Mongolia and passed through the border of Shanxi and Shaanxi, the border of western Henan and Shanxi, western Henan, and central Hubei. The trajectory was very long, and the air mass moved rapidly, but the concentrations of air pollutants carried by it were at a very low level except for O_3. Among the input pollutants, the concentrations of PM2.5 and PM10 were only 15.7 and 19.9 $\mu g/m^3$ in Changsha, 11.7 and 19.4 $\mu g/m^3$ in Zhuzhou, and 11.3 and 17.7 $\mu g/m^3$ in Xiangtan, while the concentrations of SO_2, NO_2, and O_3 were only 4.7–5.7, 6.5–9.3, and 0.4–0.6 $\mu g/m^3$, respectively. However, in February, the O_3 concentration brought by each airflow trajectory was not low; in particular, the O_3 concentration of No. 3 was above 60 $\mu g/m^3$, which was much higher than the average seasonal value.

On the whole, in winter, the airflow from northwest China carried fewer air pollutants and was relatively clean, while the airflow from the north by east and south passing through more developed areas had a higher average concentration of pollutants, and the pollution situation was relatively severe.

3.3. Analysis of Potential Source Area and Pollution Degree. In order to further analyze the air pollution transport source and confirm the potential source area of winter pollutants, the PSCF analysis of PM2.5 concentration in the study area was carried out by using MeteoInfo software. The contribution value of potential sources represents the proportion of pollution trajectories in the area. The greater the value, the more significant the contribution to PM2.5 concentration in the target study area and the greater the possibility of the region as the source of air pollution in the target area. The calculation results are shown in Figure 3.

In Figure 3, the darker the color, the greater the PSCF value. It can be seen that the PSCF value of PM2.5 in the study area has a wide span and a large coverage area, mainly concentrated in Hunan, Hubei, Jiangxi, and Henan provinces, which means that the main potential source areas of PM2.5 in the study area are concentrated in the adjacent areas of Chang-Zhu-Tan region and the surrounding developed areas.

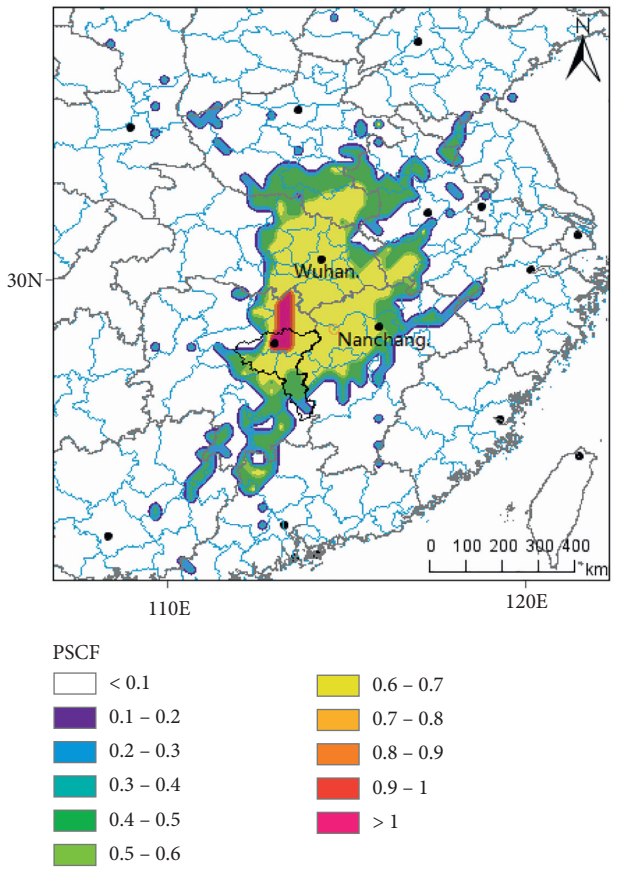

Figure 3: Contribution distribution of potential source areas of PM2.5 in winter of 2019 in Chang-Zhu-Tan region.

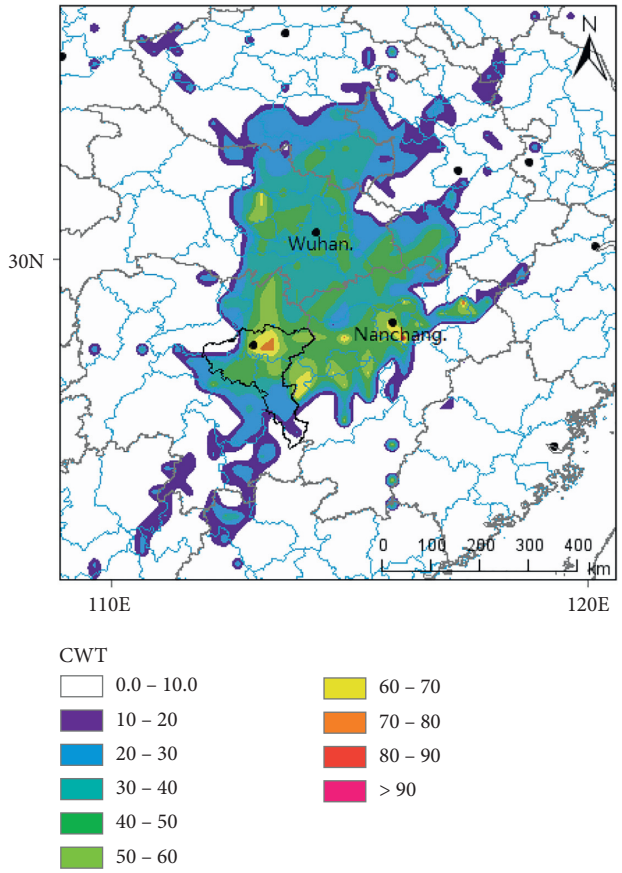

Figure 4: CWT contribution of PM2.5 in winter of 2019 in Chang-Zhu-Tan region.

The PSCF method calculates the proportion of pollution trajectories to all trajectories in a certain area to reflect the potential pollution impact of the region on the target area, which is only a conditional probability. On this basis, in order to quantitatively analyze the pollution level of different source regions, the CWT analysis method is used to calculate the weight concentration of each trajectory.

It is evident that the distribution characteristics of CWT and PSCF in winter in Chang-Zhu-Tan region are similar (Figure 4). The high-value range of CWT is concentrated in Hunan, Hubei, and Jiangxi. Unlike the distribution of PSCF high-value areas, CWT high-value areas are relatively scattered, which is not entirely centered on the study area. Hubei, Henan, Jiangxi, and Hunan are not connected to a large high-value region, so a more accurate source distribution is given. The main distribution areas are Chang-Zhu-Tan region and Yueyang city in Hunan province, Jingzhou city, and Xiaogan city in the central part of Hubei province, Ezhou region in the south of Wuhan City, Nanchang city in Jiangxi province, Pingxiang city in Jiangxi province bordering Zhuzhou city in Hunan province, central Jiangxi province (Xinyu and Ji'an city), and south of Jingdezhen in the northeast of Jiangxi. These areas are consistent with the key potential source areas analyzed by PSCF, and the contribution value of PM2.5 daily average mass concentration in the study area exceeds national secondary standard limit ($75\,\mu g/m^3$). In addition, there are also a few small areas with a high contribution, such as Ganzhou city in the south of Jiangxi province and Xinyang city in the south of Henan province.

4. Discussion

In this paper, the potential source areas of PM2.5 in the study area are obtained by PSCF method, and the contribution weights of different source areas to PM2.5 concentration are obtained by CWT method. The distribution characteristics calculated by the two methods are close. Different from the distribution of PSCF high value area, the CWT high value area is relatively scattered and not completely centered on the study area. Compared with PSCF, the potential source areas determined by CWT method are more accurate, and this result may help to formulate pollution reduction strategies. There are three reasons that lead to the main potential sources of PM2.5 concentrated in the surrounding areas of Chan-Zhu-Tan area and the surrounding developed areas. Firstly, the industries in these areas are relatively developed, and the emission of air pollutants is high [24]. Secondly, the airflow through these areas moves slowly, and pollutants easily form accumulation. Thirdly, the pollutant diffusion effect is not good due to the short distance transmission, so it has a significant impact on the study area.

Due to seasonal heating and weather patterns with concentrated pollution in low altitude areas, the concentration of pollutants in winter in China is slightly higher than that in other seasons, and most areas cannot obtain long-term station data, so we chose the data of three months in winter for research. The estimated value of particulate pollution from the current study period may be similar to or slightly higher than the long-term average. However, because remote sensing data sets usually focus on annual or multiyear averages, this limits the ability to make direct comparisons.

The future work can be divided into two parts: (1) exploring seasonal changes and long-term trends combined with remote sensing data; (2) we can continue to establish the list of major pollutant emission sources in Chang-Zhu-Tan region and use various air quality models to simulate the complex process of atmospheric particulate matter diffusion and transformation. This will help to analyze the source of atmospheric particulate matter more scientifically and accurately.

5. Conclusion

Topography analysis shows that the northeast of Chang-Zhu-Tan area is the North China Plain and the Middle-Lower Yangtze River Plain, and there is no obvious mountain barrier for the airflow from the eastern ocean to central China. In the northwest direction, there are Qilian Mountains, Qinling Mountains, and Daba Mountains. In winter, Siberian cold air flows into the interior of China and even eastern China along the southeast trending Qilian Mountains. The south is hilly, and the airflow from the East China Sea and the South China Sea flows clockwise to central China. In the north, west, and southwest, there are Loess Plateau, Qinghai Tibet Plateau, and Yunnan Guizhou Plateau, which form natural barriers to block the airflow, so there is less airflow in these directions.

During the winter of 2019, as a whole, the trend of the airflow trajectories obtained by the backward trajectories clustering of the three cities in the study area was basically the same. The cluster trajectories were consistent with the leading wind directions in the meteorological analysis, and most of them were imported from the north by west, northeast, and south by west. Because of the significant influence of topography, the airflows were mostly imported along the mountain ranges. In all kinds of clustering airflow trajectories in winter, the average concentrations of pollutants carried by the airflow trajectories imported from eastern Hubei and northeastern Hunan were the highest, especially NO_2 and PM2.5, which exceed the national daily average concentration limits. The airflow trajectories were short, and the moving speeds of air masses were slow, which were affected by the short distance transmission of human-made pollution emissions in some areas, and the atmospheric diffusion condition was poor. In addition, the study period may be affected by the epidemic situation, factory shutdown, vehicle flow reduced, emissions reduced, and all kinds of air pollutants in the route area significantly reduced.

Data Availability

The data used and/or analyzed during the current study are available from the corresponding author upon reasonable request.

Conflicts of Interest

The authors declare that they have no conflicts of interest.

Acknowledgments

The authors would like to kindly thank Ms. Li (Qiaoyun Li), Ms. Wang (Ling Wang), and Ms. Zhang (Juan Zhang) for polishing this manuscript and thank Ms. Wang (Yaru Wang) and Ms Zhou (Hui Zhou) for their contribution to this study as jointly trained students. This work was supported by the National Natural Science Foundation of China (nos. 31971456 and 31600355) and the Hunan Province Special Project of Forestry Science and Technology Innovation of China (nos. XLK202103-2 and XLK201942).

References

[1] W. X. Wang, F. H. Chai, Z. H. Ren et al., "Process, achievements and experience of air pollution control in China since the founding of the People's Republic of China 70 years ago," *Research of Environmental Sciences*, vol. 32, no. 10, pp. 1621–1635, 2019.

[2] L. Yin, L. Wang, W. Huang, S. Liu, B. Yang, and W. Zheng, "Spatiotemporal analysis of haze in Beijing based on the multi-convolution model," *Atmosphere*, vol. 12, no. 11, p. 1408, 2021.

[3] Y. Liu, J. Tian, W. Zheng, and L. Yin, "Spatial and temporal distribution characteristics of haze and pollution particles in China based on spatial statistics," *Urban Climate*, vol. 41, Article ID 101031, 2022.

[4] S. D. Liu, J. N. Shi, and Y. Cheng, "Review of pollution characteristics of PM 2.5 in Chinese representative megacities," *Research of Environmental Sciences*, vol. 33, no. 2, pp. 243–251, 2020.

[5] B. Merete, B. Kelley, B. Murray, D. Christopher, and R. Ilona, "Saturation vapor pressures and transition enthalpies of low-volatility organic molecules of atmospheric relevance: from dicarboxylic acids to complex mixtures," *Chemical Reviews*, vol. 115, no. 10, pp. 4115–4156, 2015.

[6] M. L. Acosta-Urdapilleta, E. Villegas, E. Villegas, A. Estrada-Torres, M. Téllez-Téllez, and G. Díaz-Godínez, "Antioxidant activity and proximal chemical composition of fruiting bodies of mushroom, Pleurotus spp. produced on wheat straw," *Journal of Environmental Biology*, vol. 41, no. 5, pp. 1075–1081, 2020.

[7] A. Fulvio and K. H. Philip, "Source apportionment of the ambient PM 2.5 across St. Louis using constrained positive matrix factorization," *Atmospheric Environment*, vol. 46, no. 1, pp. 329–337, 2012.

[8] Y. Liu, Y. Yu, M. Liu et al., "Characterization and source identification of PM2.5-bound polycyclic aromatic hydrocarbons (PAHs) in different seasons from Shanghai, China," *Science of The Total Environment*, vol. 644, pp. 725–735, 2018.

[9] B. Moroni, S. Crocchianti, C. Petroselli et al., "Potential source contribution function analysis of long-range transported aerosols in the central mediterranean: a comparative study of

two background sites in Italy," *Rendiconti Lincei. Scienze Fisiche e Naturali*, vol. 30, no. 2, pp. 337–349, 2019.

[10] Y. Wang, H. Wang, and S. Zhang, "A weighted higher-order network analysis of fine particulate matter (PM2.5) transport in Yangtze River Delta," *Physica A: Statistical Mechanics and its Applications*, vol. 496, no. 3, pp. 654–662, 2018.

[11] Z. D. Zhang, T. J. Shao, X. G. Huang, and P. R. Wei, "Characteristics and potential sources of PM 2.5 pollution in Beijing-Tianjin-Hebei region in 2017," *Environmental Engineering*, vol. 38, no. 2, pp. 99–106, 2020.

[12] F. R. Deng, N. Kang, H. Kang, Y. C. Jiang, and Y. Xing, "Analysis of air pollution episodes over different cities in the Yangtze River Delta," *China Environmental Science*, vol. 38, no. 2, pp. 401–411, 2018.

[13] E. Potier, A. Waked, A. Bourin et al., "Characterizing the regional contribution to PM10 pollution over northern France using two complementary approaches: Chemistry transport and trajectory-based receptor models," *Atmospheric Research*, vol. 223, pp. 1–14, 2019.

[14] P. Praphatsorn and C. Somporn, "Identification of potential sources of PM 10 pollution from biomass burning in northern Thailand using statistical analysis of trajectories," *Atmospheric Pollution Research*, vol. 9, no. 6, pp. 1038–1051, 2018.

[15] K. Yang, Q. Li, M. Yuan et al., "Temporal variations and potential sources of organophosphate esters in PM2.5 in Xinxiang, North China," *Chemosphere*, vol. 215, pp. 500–506, 2019.

[16] C. L. Zhu, S. S. Meng, and R. G. Zhang, "Correlation analysis and spatial and temporal distribution characteris of main atmospheric pollutants in Xi'an," *Environmental Engineering*, vol. 35, no. 12, pp. 86–91, 2017.

[17] K. Peng, Y. Yang, J. Y. Zheng, S. S. Yin, Z. J. Gao, and X. B. Huang, "Emission factor and inventory of paved road fugitive dust sources in the Pearl River Delta region," *Acta Scientiae Circumstantiae*, vol. 33, no. 10, pp. 2657–2663, 2013.

[18] X. Zhou, T. J. Zhang, Z. Q. Li, Y. Tao, and F. T. Wang, "Particulate and gaseous pollutants in a petrochemical industrialized valley city, Western China during 2013–2016," *Environmental Science and Pollution Research*, vol. 25, no. 15, pp. 15174–15190, 2018.

[19] R. A. Rohde and R. A. Muller, "Air pollution in China: mapping of concentrations and sources," *PLoS One*, vol. 10, no. 8, Article ID e0135749, 2015.

[20] Y. Chen, S. Xie, and B. Luo, "Seasonal variations of transport pathways and potential sources of PM2.5 in Chengdu, China (2012-2013)," *Frontiers of Environmental Science & Engineering*, vol. 12, no. 1, p. 12, 2018.

[21] Y. Li, *Study on Land Use Change and its Effects on Eco-Environment in CZT Core Region*, Dissertation, Hunan Agricultural University, Changsha, Hunan, China, 2015.

[22] C. Yang, F. Gao, and M. Dong, "Energy efficiency modeling of integrated energy system in coastal areas," *Journal of Coastal Research*, vol. 103, no. 1, p. 995, 2020.

[23] J. Li, N. Chen, Y. Zhao, M. Liu, and W. Wang, "A catastrophic landslide triggered debris flow in China's Yigong: factors, dynamic processes, and tendency," *Earth Sciences Research Journal*, vol. 24, no. 1, pp. 71–82, 2020.

[24] L. He, Y. Chen, and J. Li, "A three-level framework for balancing the tradeoffs among the energy, water, and air-emission implications within the life-cycle shale gas supply chains," *Resources, Conservation and Recycling*, vol. 133, pp. 206–228, 2018.